



Photocatalytic oxidation of aqueous naproxen with a horizontally placed solar CPC slurry reactor

Perla Patricia Hernández-Colorado^a, Sandra Pinto^b, Julio César Morales-Mejía^{b,*}, Yolanda Marina Vargas-Rodríguez^b, Graciela Ruth Delgadillo García^b, Rafael Almanza^a

^aUniversidad Nacional Autónoma de México, Instituto de Ingeniería, Coordinación de Mecánica y Energía. Av. Universidad 3000, Universidad Nacional Autónoma de México, 04510, Coyoacán, Mexico, Tel. +52 55 56233600 Ext. 3689; emails perla_patyhdz@yahoo.com (P.P. Hernández-Colorado), ras@pumas.iingen.unam.mx (R. Almanza)

^bUniversidad Nacional Autónoma de México, Facultad de Estudios Superiores Cuautitlán. Av. 1^o de mayo s/n, Infonavit Centro, 54760, Cuautitlán Izcalli, Mexico, Tel. +52-555-6232025; emails: mmjc_80@yahoo.com.mx (J.C. Morales-Mejía), fairylove_9@hotmail.com (S. Pinto), Tel. +52-555-6239431; email: ym_vargas@yahoo.com.mx (Y.M. Vargas-Rodríguez), Tel. +52-555-6232002; email: gradel0608@hotmail.com (G.R. Delgadillo García)

Received 8 September 2015; Accepted 19 November 2016

ABSTRACT

A solar photocatalytic reactor, that includes a horizontal compound parabolic collector (CPC) with a unitary geometrical concentration ratio, was designed, built and tested. The reactor was used for the photocatalytic oxidation of aqueous naproxen (NPX) with solar UV irradiance. NPX ($C_o = 10$ mg/L) and its intermediate products were monitored by UV-Vis spectrophotometry after filtering the samples. This target molecule was effectively removed when solar irradiance, Evonik P25 TiO₂ and persulfate were used together. No intermediate products remained at important concentrations at the end of the reactions. The reaction kinetics fit partially to a pseudo-first-order Langmuir-Hinshelwood kinetic model. NPX and its intermediate compounds were removed with global efficiencies of up to 99%. These results indicate that the TiO₂-based photocatalytic reactor, with a good optical design for the CPC collectors, can be effective in detoxifying polluted waters.

Keywords: CPC; Degussa P25; Contaminants of emerging concern; Naproxen; Photocatalysis; TiO₂

1. Introduction

Recently, there has been growing interest in advanced water and wastewater treatment technologies, which are required when pollutants remain present in water after conventional treatment operations [1]. Some pollutants remain in conventionally treated waters because they are not biodegradable, whereas others are present at very low concentrations; sometimes both of these scenarios occur. Organic pollutant oxidation by heterogeneous photocatalysis is one of the most interesting and promising applications of photochemistry in water treatment because of the non-selective nature of heterogeneous photocatalysis (which can be applied to treat water

containing complex mixtures of pollutants) and because solar radiation is a free source of energy with which to activate the catalyst, an important environmental advantage [2].

Heterogeneous photocatalysis is one of the new advanced oxidation technologies for wastewater treatment that is based on the high oxidation potential of hydroxyl radicals [1,3,4] in the oxidation of organic molecules. The mechanism, reaction paths and oxidation kinetics of heterogeneous photocatalysis in aqueous media have been widely described in the literature [3–7]. The process is based on the chemical reactivity of a photohole and photoelectron, and it is important to consider that the photoelectrons must react as fast as possible with an oxidizer (dissolved oxygen, hydrogen peroxide, persulfate, etc.) in order to avoid their recombination with the

* Corresponding author.

photoholes and to eventually generate additional radicals. The Langmuir–Hinshelwood (L–H) kinetic model has been widely employed (Eq. (1)) to describe these reactions and can be simplified when the initial concentration of the pollutant is low enough, giving Eq. (2). If the kinetics are based on the ultraviolet A (UVA) energy dose ($E_{\text{UVA,acc}}$) instead of the reaction time, r can be defined as $dC/dE_{\text{UVA,acc}}$; then, k and k_{app} must be renamed as k_E and $k_{\text{app},E'}$ respectively.

$$r = k \cdot \theta = \frac{k \cdot K \cdot C}{1 + K \cdot C} \quad (1)$$

$$r = \frac{k \cdot K \cdot C}{1 + K \cdot C} \approx \frac{k \cdot K \cdot C}{1} \approx k \cdot K \cdot C \approx k_{\text{app}} C \quad (2)$$

When titanium dioxide is used as a catalyst, the solar UVA irradiance can be effectively utilized. Roughly stated, approximately 3.5% of the global solar irradiance spectrum is comprised of UVA energy [8,9], and horizontal UVA irradiance can reach values as high as 42 W/m² during a typical clear-sky day in Mexico City (in summer). This amount of useful solar energy makes solar photocatalytic oxidation suitable for water purification. Of the available photocatalytic treatment options, such as modifications to titanium dioxide and the use of other catalysts (allowing the use of visible light for photocatalytic oxidation), pure titanium dioxide (mainly the anatase crystalline phase, such as Evonik P25 nanopowders) is the most important catalyst due to its photonic efficiency, which reportedly decreases when TiO₂ is doped or modified [10,11]. In addition, titanium dioxide is the most promising option because of its high chemical stability against water and radiation, low cost and excellent chemical and photonic efficiencies.

Naproxen (NPX; (+)-(S)-2-(6-methoxynaphthalen-2-yl)propanoic acid), as well as its water-soluble sodium salt, is a member of the non-steroidal anti-inflammatory drugs (NSAIDs) family with analgesic and antipyretic properties and is widely used to treat pain, fever, inflammation and stiffness. NPX is considered as an environmentally persistent compound because of its continuous discharge to water bodies in wastewater emissions. NSAIDs, such as NPX, have been found in water, soil and sediments at concentrations from nanograms to micrograms per liter [12,13] and are contaminants of emerging concern. In addition, ecotoxicological studies have shown that intermediate and final products from environmental transformations of NPX can be more toxic than the parent compound, such as those reported by Isidori et al. [14] and DellaGreca et al. [15]. NPX has two aromatic rings and strong absorbance peaks in the range of 220–280 nm.

Heterogeneous photocatalysis can be performed inside tubular solar reactors that use curved mirrors to concentrate and distribute radiation around a UV-transparent pipe. One option is the use of low-concentration compound parabolic collectors (CPCs), which are static solar reflecting devices of which the optic allows reaching the maximum theoretical capture of incident photons that reach its aperture with an angle less than or equal to half of its acceptance angle and then reflecting those photons to the tubular absorber or reactor. If the CPC collector has a unitary geometrical concentration ratio (CRg), the device can effectively use either direct or diffuse irradiance, which is an excellent option for places

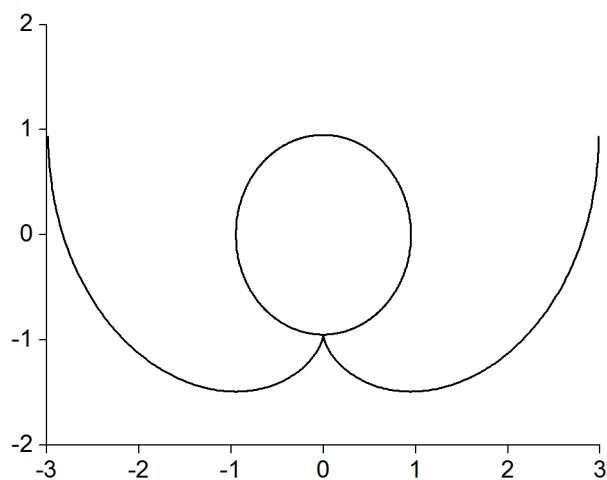


Fig. 1. Profile curve for a CPC collector with a geometrical concentration ratio of 1 and a cylindrical receptor.

where cloudiness is frequent. Solar UV irradiance on cloudy days can be composed of up to 50% diffuse photons; therefore, the use of CPC with unitary CRg could be an important advantage over several other concentrating devices for photocatalysis [16]. The design equations of these CPC collectors are the parametric expressions presented by Baum and Gordon [17] and Winston et al. [18] (Fig. 1).

At locations with low latitudes and/or during the summer (such as Mexico City), the UVA irradiance on horizontal planes is considerably higher than that on tilted planes pointing toward the south (or the north if the reactor is located on the southern hemisphere) because the solar altitude can be greater than 90° [2,19]; photocatalytic reactors with CPC collectors (CRg = 1) placed horizontally during summer and tilted (south facing) during winter must result in high oxidation efficiencies.

Although there have been many studies on the photocatalytic oxidation of contaminants of emerging concern, studies focused on NPX plus the use of a reactor with solar UVA irradiance and horizontal CPC collectors (unitary CRg) have not been reported. This paper presents the results obtained for the photocatalytic oxidation of this drug in a solar horizontal CPC reactor at several initial pH values and persulfate concentrations without a previous adsorption period of the pollutant on the catalyst. Additionally, the main intermediate compounds were determined by GC–MS.

2. Methods

The study was divided into two stages: first, catalyst elaboration and characterization; second, experimental tests for photocatalytic removal of NPX. The catalyst for the tests with TiO₂ as a slurry was Aerioxide P25 nanopowder (Evonik Industries, Essen, Germany). In addition, soda-lime glass spheres were covered by a TiO₂ film by a conventional sol-gel process reported elsewhere [20–22]. The spheres were covered by immersion, first with two SiO₂ layers and second by five TiO₂ layers, according to the method described by Novotna et al. [22]. The TiO₂ films were sintered in a Lindberg-Sola Basic oven for 4 h at 605°C under atmospheric

conditions for the first four layers. The spheres had a five-TiO₂-layered film, with annealing for 12 h at 605°C for the last layer. The precursors for the films had the following molar ratios: 10:1:0.1 (ethanol:tetraethyl orthosilicate:H⁺) and 1:62.5:0.6:8.8:0.04 (titanium tert-butoxide:ethanol:acetyl acetone:water:H⁺).

The chemicals (analytical reagent grade) were all purchased from Sigma-Aldrich (Toluca, Mexico) and used without further purification.

2.1. Film characterization and chemical analysis

The TiO₂ films deposited on spheres were characterized by X-ray diffraction (XRD; Siemens D5000, Ni filter, Cu K α radiation [$\lambda = 1.7903 \text{ \AA}$]), field emission scanning electron microscopy (FESEM; JEOL JSM5600), energy-dispersive spectroscopy (EDS; Oxford INCA, X-ACT) and Raman spectroscopy (Nicolet Almega XR, Nd:YVO₄ laser [532 nm], 25 mW). The thickness of TiO₂ films was estimated with a Leica-Cambridge S440 scanning electron microscope operating at an accelerating voltage of 2 kV. The Degussa P25 nanopowder was not analyzed because its properties have been published elsewhere [23–25].

NPX and its intermediate oxidation products from the experiments were monitored by a UV-Vis spectrophotometer

(UV1601, Shimadzu, Japan). Samples were collected from the reservoir (Fig. 2) at fixed reaction times and filtered through a cellulose syringe filter (Millipore, 0.45 μm pore) before their spectral absorbance was quantified. The measurement wavelength range was 200–800 nm. Kinetic analysis was performed with the absorbance data around the peaks at 230 and 272 nm because aromatic rings typically absorb at approximately 260–280 nm (UV absorbing species are measured at 254 nm according to AWWA/APHA Standard Methods [26]), and the substituents of NPX contribute to the absorbance at wavelengths of approximately 200–240 nm [27]. Additionally, GC-MS studies were carried out in order to determine the main intermediate compounds (Agilent 6890N, split/splitless injector, capillary HP-5MS column), for which organic molecules were previously extracted with ethyl acetate. The injector temperature was 250°C in split mode, the column temperature cycle started at 150°C and increased at 15°C per minute to 300°C. Helium was used as the carrier gas at a flow rate of 1 mL per minute. The MS detector was an Agilent model 5973, and the temperatures of the MS source, MS quad and detector were 230°C, 150°C and 75°C, respectively. Analyses were performed by electronic impact (70 eV).

The UVA solar irradiance was measured with either a portable UVA radiometer (YK35UV, Lutron, Taiwan) in situ on the reactor plane or a total ultraviolet radiometer (Eppley TUVR, USA). For laboratory tests, the solar simulator (Atlas, Suntest XLS, USA) directly recorded and exported the UVA irradiance and UVA energy dose.

The TiO₂ films characterization was divided into non-photocatalytic reactions and photocatalytic reactions, as follows.

2.2. Photocatalytic reactors and devices

A tubular reactor without any reflecting surfaces and with a Pyrex pipe (24 mm diameter, 1.5 mm thickness and six sections 250 mm in length each) was employed. For the preliminary photocatalytic tests, a CPC reactor (CR_g = 1) was designed, built and employed (Fig. 2(A)). In this reactor, the Pyrex pipe was 25 mm in external diameter, 1.5 mm thick and 300 mm in length for each pass (two passes; mean hydraulic residence time: 2 s). In these two sets of laboratory tests, the UVA irradiance was provided by the solar simulator and was fixed at 70 W/m². Their total treated volume was 1 L. These two reactors were operated in batch mode.

A pilot solar photocatalytic reactor based on two identical CPC collectors in parallel was designed, constructed and tested (Fig. 2(B)). Each CPC collector had a unitary CR_g, a Pyrex cylindrical reactor (19 mm diameter, 1 mm wall thickness, 1,000 mm length). The reactor was horizontally placed and connected to a vertical tank of variable volume (from 2 up to 20 L). For the present work, the total water volume was set at 2.2 L. Water and a TiO₂ slurry were recirculated with a small electric pump at a rate of 4.8 L/min (mean hydraulic residence time: 8.8 s). This CPC reactor was operated in batch mode.

2.3. Preliminary non-photocatalytic experiments

Adsorption, photolysis and chemical oxidation tests were first performed in the laboratory in order to determine whether these processes were important for the photocatalytic removal of NPX. The adsorption tests were carried out with 1 L of NPX solutions, 0.1 g/L TiO₂ and three initial

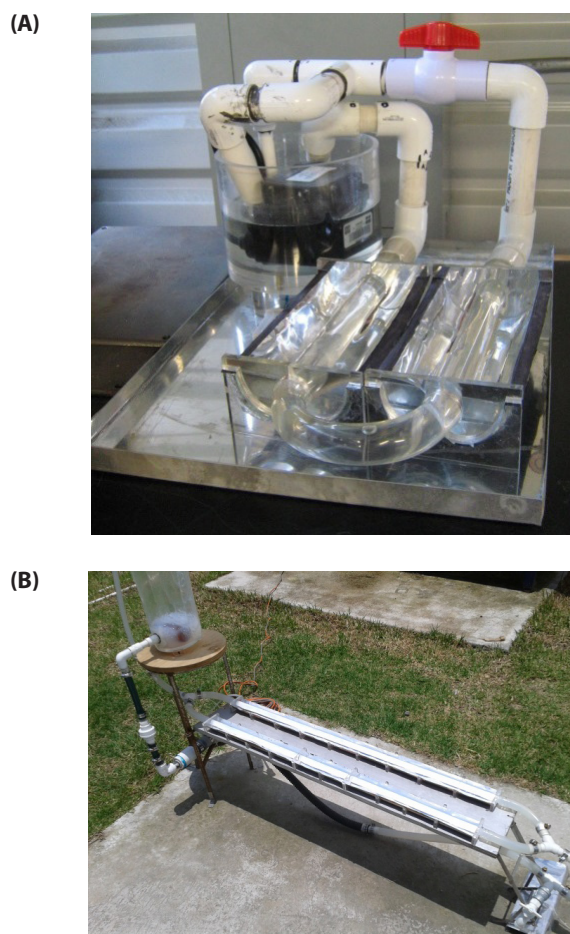


Fig. 2. CPC photocatalytic reactors: laboratory reactor (A) and solar reactor (B).

concentrations of NPX (5.53, 9.25 and 28.21 mg/L) under vigorous mixing in the dark. The photolysis tests were performed under 70 W/m² UVA irradiance, starting with 10 mg/L NPX. The chemical oxidation tests consisted only of exposing NPX ($C_0 = 10$ mg/L) solutions to persulfate ($C_0 = 0.001$ M) in the dark and without TiO₂. A combination of photolysis and chemical oxidation was carried out with 10 mg/L NPX (70 W/m² UVA irradiance, 0.001 M initial persulfate concentration) in order to determine if there was a synergistic contribution from these processes.

2.4. Photocatalytic experiments

Pilot-scale experiments were performed during summer at Ciudad Universitaria, Coyoacán, Mexico City (Table 1). The pilot reactor was operated with $Re = 2,995.9$ on each Pyrex pipe (transition flow regime) and was installed and tested at the Solar Plant of the Engineering Institute of UNAM (19°19'29.98" N, 99°11'8.16" W). For all of the photocatalytic oxidation experiments, there was no previous adsorption period so that the concentration gradient (liquid and catalyst surface) was as high as possible during the course of the reaction. NPX solutions were recirculated continuously from CPC reactor to a reservoir and samples were taken periodically, filtered (Millipore, 0.45 μm syringe filter) and analyzed with the UV–Vis spectrophotometer (absorbance scans at wavelengths from 190 to 1,000 nm).

A set of experiments was performed to compare the effect of tilting the reactor. These tests were done with the small reactor (see section 2.2 and Fig. 2(A)) under solar irradiance.

3. Results and discussion

3.1. TiO₂ film characterization

The Raman bands of the films (Fig. 3(A)) perfectly matched those reported for anatase TiO₂ by Arsov et al. [28] and Ma et al. [29] at 309–402 and 641–642 cm⁻¹. The XRD pattern (Fig. 3(B)) exhibited the characteristic reflections of anatase and rutile at 25.3°, 37.9°, 48.1°, 53.9° and 55.1° 2θ for anatase and at 27.5°, 36.2°, 41.4°, 54.4°, 52.8° and 64.2° 2θ for rutile, as presented by Howard et al. [30]. The particle sizes of the samples were determined by the X-ray line broadening method using the Scherrer equation with $D = (k\lambda/\beta_D \cos\theta)$, where D is the particle size in nanometers, λ is the wavelength of the radiation (1.54056 Å for Cu Kα

radiation), k is a constant equal to 0.9, β_D is the peak width at half-maximum intensity and θ is the peak position. The crystal size was 53.69 and 53.88 nm, respectively, for anatase and rutile. From SEM studies, film thickness on covered spheres ranged from 7.28 to 10 μm, with a porous morphology (Fig. 4(A)).

Fig. 4(A) presents the FESEM image of the spheres, in which the wide size distribution of the particles can be

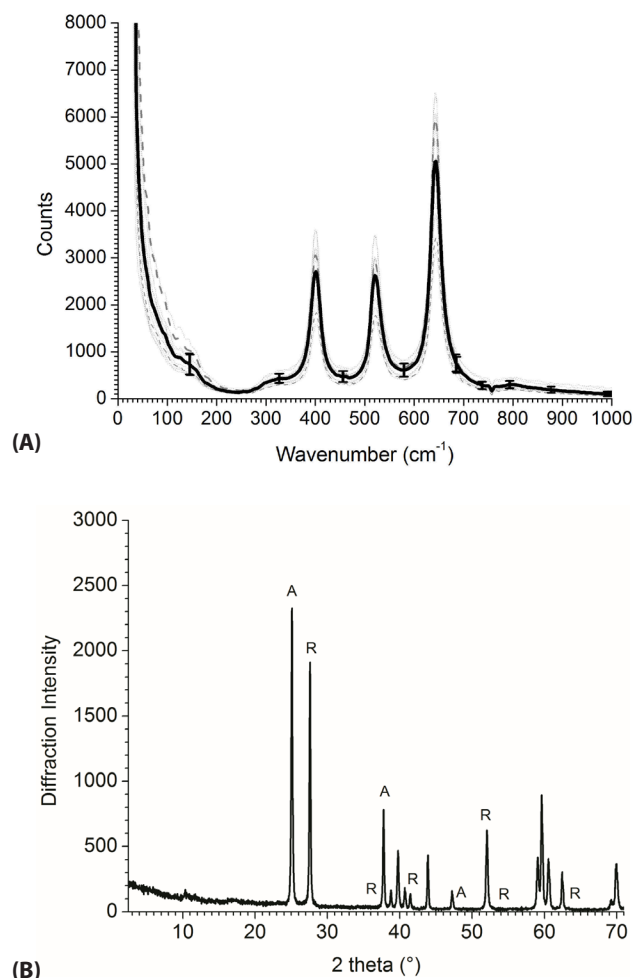


Fig. 3. Raman bands (A) and XRD diffraction intensities (B) for several film samples (five layers of TiO₂).

Table 1
Photocatalytic experiments

Parameter	Laboratory reactors	Solar pilot reactor
Initial TiO ₂ concentration and configuration	(a) 0.1 g/L, slurry (b) The amount fixed on a film on glass spheres (10 mm diameter)	0.1 g/L, slurry (a) Tilted and horizontal reactor (comparative) (b) Horizontal reactor
Initial pH	Neutral (7.5)	4, 6, 7.5, 10
Temperature control	No temperature control	No temperature control
Initial persulfate concentration (M)	0, 0.0005, 0.001, 0.005, 0.01	0, 0.0005, 0.001, 0.005
Water flow (L/s)	0.142 (CPC reactor) and 0.170 (tubular reactor)	0.08
UVA irradiance	70 W/m ²	Solar

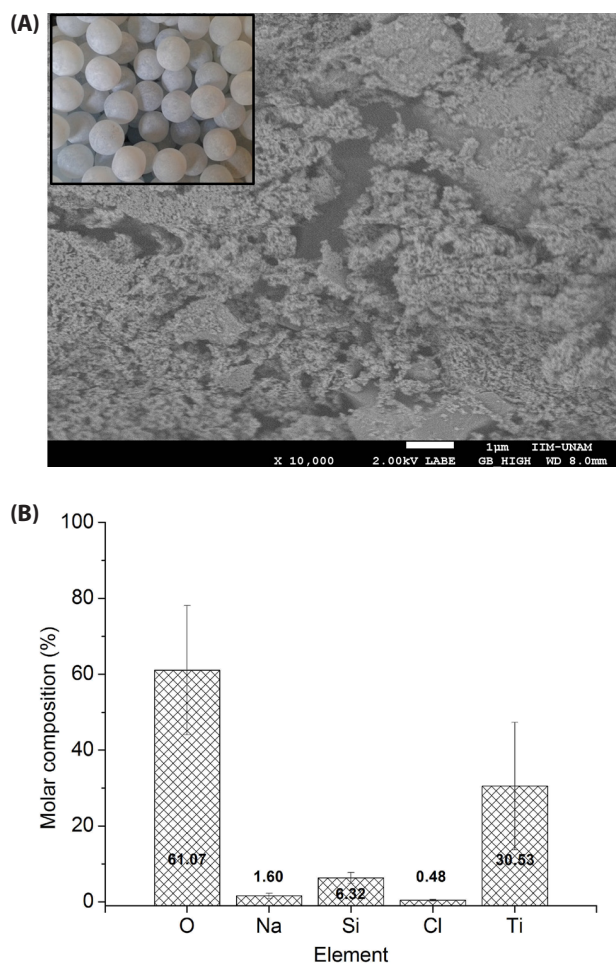


Fig. 4. FESEM image of the TiO_2 film, with an inset photo of the covered spheres (A), and the average composition (B) of a typical film based on EDS.

observed. The particle sizes oscillated around a few nanometers. EDS analysis of four samples (Fig. 4(B)) indicates that the films were composed of O, Ti, Si, Cl and Na (Fig. 4(A)). The Na and Cl ions were attributed to the glass composition because the EDS detector analyzes the samples from the surface to several micrometers depth. The Si and O atoms mainly correspond to the SiO_2 layer. This information indicates that the main components near the surface of the films were TiO_2 , SiO_2 , NaCl and Na_2O .

3.2. Preliminary non-photocatalytic experiments

The maximum reduction of NPX by adsorption on TiO_2 was achieved for $C_0 = 5.52 \text{ mg/L}$, being as high as 20% after 2,880 min. For the other two initial concentrations of NPX (9.25 and 28.21 mg/L), the adsorptions were only 6% and 17%, respectively. Considering this behavior, adsorption is not expected to play an important role in the removal efficiencies of NPX compared with photocatalytic oxidation when the total reaction times are considerably lower than 2,880 min; of course, adsorption is an important step in the reaction mechanism of heterogeneous photocatalytic oxidation [2,31].

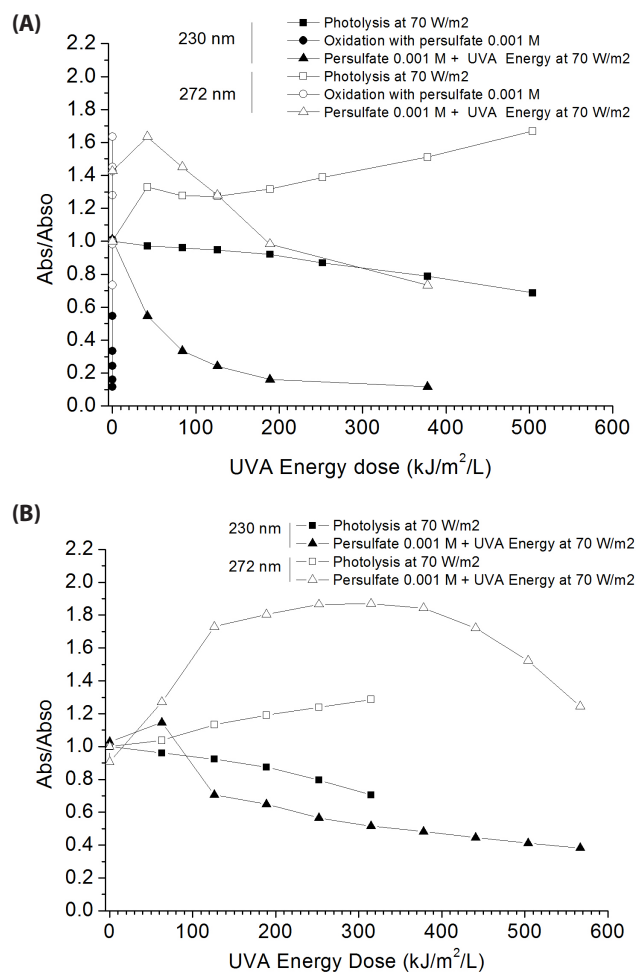


Fig. 5. Non-photocatalytic reactions of NPX in the tubular (A) and CPC (B) reactors at neutral pH.

Figs. 5(A) and (B) show that the absorbance at 230 nm decreased during the non-photocatalytic tests (photolysis, chemical oxidation and the combination of these processes). On the other hand, the absorbance increased at 272 nm during first stages of the reactions, then reached a maximum and decreased after receiving sufficient UVA energy. This behavior might indicate that the initial intermediate molecules formed during the first steps of these reactions were species that absorb energy in the UV range and could be based on the NPX skeleton. These intermediate species are expected to be slowly phototransformed into non-absorbing species in the beginning. The only exception to this behavior was for photolysis, for which the absorbance at 272 nm did not decrease during the entire test, which indicates that the NPX molecule was not easily broken by photolysis. This result agrees with the works of DellaGrecia et al. [15], Arany et al. [32], Marotta et al. [33] and Musa and Eriksson [34], who stated that the main transformation of NPX by photolysis mainly generates molecules that are only partially oxidized, with the NPX skeleton unchanged, and/or a mixture of two NPX molecules. All of the species that these researchers reported or suggested must absorb at similar wavelengths as NPX due to the two-ring skeleton

that they have in common. These results also indicate that the non-photocatalytic reactions were faster with the tubular reactor. We believe that this is due to the differences in the exposed areas of the reactors: 0.0565 m² for the tubular reactor and 0.0236 m² for the CPC reactor.

On the basis of these results, effective removal of NPX and absorbing species by non-photocatalytic processes was achieved with persulfate oxidation and with the simultaneous use of persulfate anions and UVA irradiance.

3.3. Laboratory photocatalytic experiments

The results of laboratory experiments on heterogeneous photocatalytic oxidation are displayed in Fig. 6 for different initial persulfate concentrations and two catalyst forms. The absorbance at 230 and 272 nm was the initial choice for kinetic analysis. The absorbance at 272 nm increased during the initial moments of the photocatalytic oxidation, reached a maximum and then decreased with L–H pseudo-first-order kinetics; on the other hand, the absorbance at 230 nm decreased from the beginning of the reactions but did not show a good fit with the proposed kinetics. We reasoned that this result could be a consequence of the chemical nature of the intermediate compounds because they are based on the NPX skeleton with added hydroxyl groups (from hydroxyl radicals) and, eventually, on the decarboxylated and demethylated derivatives of NPX, as has been proposed by Marotta et al. [33] and Zhang et al. [35].

The TiO₂ films on spheres removed smaller amounts of NPX compared with the P25 nanopowders (Fig. 6), which is congruent with the explanations of Herrmann [3,31] and Blanco [2] involving the negative influence of the smaller surface areas that films typically have in comparison with nanopowders. Because of this behavior, P25 was chosen to perform all of the solar oxidation photocatalytic experiments. In addition, persulfate has an effect on NPX oxidation: the best initial concentration was 0.001 M for the experiments performed at laboratory with solar simulator when P25 nanopowders were used.

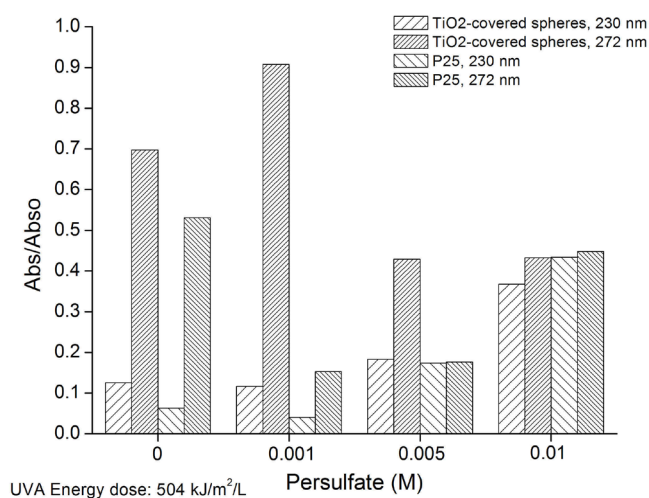


Fig. 6. Photocatalytic oxidation of NPX with a CPC reactor and solar simulator (70 W/m²/L) at neutral pH.

3.4. Solar photocatalytic experiments

We performed a comparison of the slope of the CPC collector on the performance of the reactor ($V_0 = 1$ L; $C_0 = 10$ ppm; 0.1 g/L of P25 nanopowder; persulfate initial concentration = 0.001 M). The results are presented in Fig. 7. It is clear that having the CPC horizontally placed resulted on higher efficiency of NPX oxidation and in a smaller amount of initial intermediates.

The kinetics was analyzed in order to determine the fit to the pseudo-first-order L–H model ($k_{app,E}$) or to the original unmodified L–H model (k_E) presented in Eqs. (1) and (2). In Fig. 8, the resulting k_E values for all of the solar photocatalytic reactions for the four different initial pH values and persulfate concentrations are presented. In contrast, in Fig. 9, $k_{app,E}$ can be observed when the reaction kinetics were fitted to the pseudo-first-order L–H simplification, separating the reactions for the kinetics fitting around the inflection point of the Abs/Abs₀ curves (not presented), which produced two values of $k_{app,E}$ for each of the reactions ($k_{app,E-1}$ and $k_{app,E-2}$). As reported

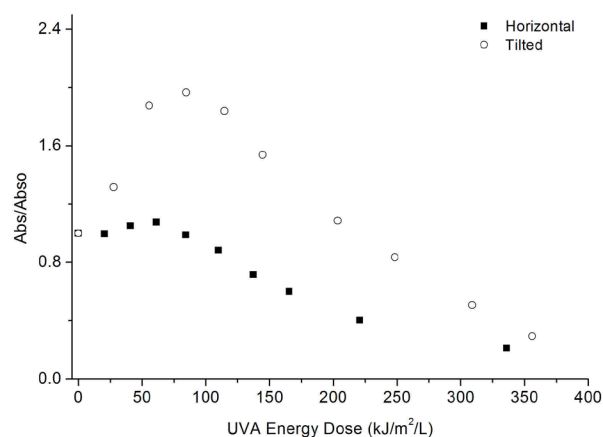


Fig. 7. Effect of CPC collector slope on naproxen removal under solar irradiance.

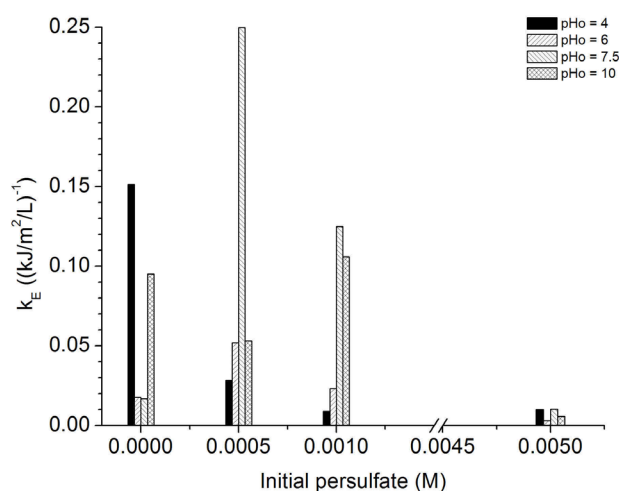


Fig. 8. Kinetic constants k_E for the solar photocatalytic oxidation of NPX.

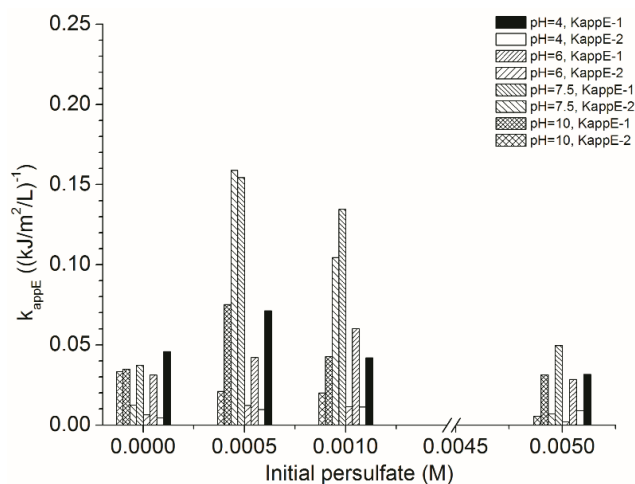


Fig. 9. Kinetic constants $k_{app,E}$ for the solar photocatalytic oxidation of NPX.

previously [36–38], the apparent first-order kinetic constant k_{app} for the photocatalytic oxidation of NPX by TiO_2 ranges from 0.007 to $0.491 \cdot \text{min}^{-1}$, depending on irradiation source, pH conditions, electron acceptor and initial NPX concentration. These reported k_{app} values could not be easily compared with the results obtained in the present research because the former are based on a time frame (in minutes) and the latter are based on a UVA energy dose ($\text{kJ}/\text{m}^2/\text{L}$). The authors considered that the UVA energy received by the reactors must be employed in kinetics analysis because the amount of photons irradiated on the reactor is not directly related to time when the irradiance intensity is time dependent (as in solar photocatalysis), but several studies performed with UVA lamps did not include this transformation. In addition, some of the previously reported studies [36–38] presented the same behavior in plots of Abs/Abs_0 against time (proportional to the UVA energy dose) as that obtained in the present research. We consider that they may have analyzed the first moments of the reactions, when the transformation rates were the fastest.

The removal efficiencies were taken into account because this is a simpler way to choose the process conditions. The NPX removal efficiencies reached 99% (Fig. 10), depending on the initial pH level and persulfate concentration. The best conditions for the photocatalytic oxidation of NPX with the horizontal CPC reactor were an initial neutral pH with 0.0005 M persulfate, followed, in decreasing order, by pH 10, 6 and 4 with 0.0005 M persulfate.

3.5. Intermediate analysis

After extracting with ethyl acetate, the MS analysis indicated that six photoderived compounds were present in the treated water, as presented in Table 2.

Notably, all these intermediated molecules have the basic structure of naphthalene and have been found in other photocatalysis and photolysis experiments. Particularly, Marotta et al. [33] observed the first two molecules listed in Table 2 and also reported that these compounds absorb light at the same wavelength as NPX. The first intermediate also has a higher molar absorptivity than NPX.

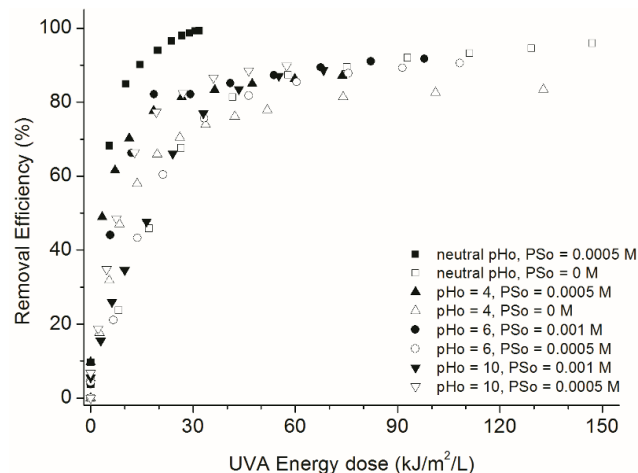
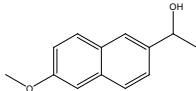
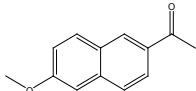
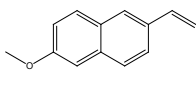
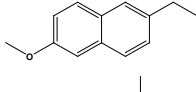
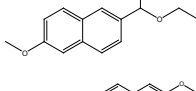
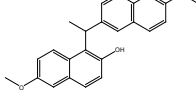


Fig. 10. NPX removal efficiencies (230 nm) for selected solar photocatalytic experiments.

Table 2

Photoderived intermediate compounds experimentally determined by GC–MS

Molecule	Name	Congruence with reported results
	2-(1-Hydroxyethyl)-6-methoxynaphthalene	Jallouli et al. [39] Marotta et al. [33] DellaGreca et al. [15] Isidori et al. [40]
	2-(1-Oxoethyl)-6-methoxynaphthalene	Jallouli et al. [39] Arany et al. [32] Marotta et al. [33] DellaGreca et al. [15] Isidori et al. [40]
	2-Ethenyl-6-methoxynaphthalene	Arany et al. [32] DellaGreca et al. [15]
	2-Ethyl-6-methoxynaphthalene	Jallouli et al. [39]
	1-Ethoxy-1-(6-methoxynaphthalen-2-yl)ethane	DellaGreca et al. [15] Isidori et al. [40]
	1-(2-Hydroxy-6-methoxynaphthalenyl)-1-(6-methoxynaphthalen-1-yl)ethane	Isidori et al. [40]

Conclusions

- The TiO_2 films prepared on spheres oxidized NPX with lower efficiency than P25 nanopowder. This result could be due to the smaller specific area and different anatase and rutile crystalline phases present, although the films presented both of these phases and a porous structure.

- The solar photocatalytic oxidation of NPX in a horizontal CPC reactor with a unitary geometric concentration ratio presented removal efficiencies as high as 99%.
- The kinetics acceptably fit to either a simplified or unaltered L–H model. In the latter model, the reactions had to be divided into two periods, before and after the inflection point on the plots of the Abs/Abs_0 vs. the UVA energy dose, in order to maintain a good fit to this classic model.
- The best reaction conditions for the solar photocatalytic oxidation of NPX in the CPC reactor were an initial neutral pH (7.5) and 0.0005 M persulfate concentration. The reaction under these conditions presented the highest kinetic constants ($k_E = 0.25$ kJ/m²/L; $k_{app,E-1} \approx k_{app,E-2} = 0.15$ kJ/m²/L) and the best efficiencies of NPX removal with the smallest amount of energy consumption (30 kJ/m²/L).
- Although intermediate compounds were present, their concentrations decreased over the course of the tests, and they were removed efficiently at the end.

Acknowledgments

Financial support for this work was provided by UNAM-DGAPA thorough PAPIIT projects IN111416 (Acondicionamiento fotoquímico-fototérmico solar de agua para uso industrial) and IA106216 (Tratamiento fotocatalítico solar de agua con contaminantes no biodegradables tipo ECP encontrados en México). The authors acknowledge Ana L. Fernandez at the Laboratorio de Difraccion de Rayos X from FES Cuautitlan for her invaluable help with the XRD analysis and Omar Novelo for his help with the FESEM and EDS studies. Additionally, P.P. Hernández-Colorado and S. Pinto thank UNAM-DGAPA and CONACyT for the scholarships.

References

- [1] G. Tchobanoglous, H.D. Stensel, R. Tsuchihashi, F. Burton, Wastewater Engineering: Treatment and Resource Recovery, 5th ed., Metcalf & Eddy, McGraw Hill, USA, 2013.
- [2] J. Blanco, Development of CPC Solar Collectors for Applications Photochemical Degradation of Persistent Pollutants in Water, Collections Ciemat, Ministry of Science and Culture, Spain, 2003.
- [3] J.M. Herrmann, Heterogeneous photocatalysis: state of the art and present applications, *Top. Catal.*, 34 (2005) 49–65.
- [4] G. Li Puma, Dimensionless analysis of photocatalytic reactors using suspended solid photocatalysts, *Chem. Eng. Res. Des.*, 83 (2005) 820–826.
- [5] J. Araña, C.F. Rodríguez, J.A.H. Melián, O.G. Díaz, J.P. Peña, Comparative study of photocatalytic degradation mechanisms of pyrimethanil, triadimenol, and resorcinol, *J. Solar Energy Eng.*, 130 (2008) 1–8.
- [6] D. Friedmann, C. Mendive, D. Bahnemann, TiO₂ for water treatment: parameters affecting the kinetics and mechanisms of photocatalysis, *Appl. Catal., B*, 99 (2010) 398–406.
- [7] S. Banerjee, S.C. Pillai, P. Falaras, K.E. O’Shea, J.A. Byrne, D.D. Dionysiou, New insights into the mechanism of visible light photocatalysis, *J. Phys. Chem. Lett.*, 5 (2014) 2543–2554.
- [8] L.A. Quiñonez, R. Almanza, Preliminary Model of Radiation UV for the Mexican Republic, First Symposium Processes Advanced Oxidation Plants, Institute of Engineering, Mexico D.F., Memories, UNAM, 2013.
- [9] B. Duffie, *Solar Engineering of Thermal Processes*, 2nd ed., Wiley Interscience, USA, 1991.
- [10] F. Fresno, C. Guillard, J.M. Coronado, J.M. Chovelon, D. Tudela, J. Soria, J.M. Herrmann, Photocatalytic degradation of a sulfonyleurea herbicide over pure and tin-doped TiO₂ photocatalysts, *J. Photochem. Photobiol., A*, 173 (2005) 13–20.
- [11] L. Rizzo, S. Merica, M. Guida, D. Kassinos, V. Belgiorno, Heterogenous photocatalytic degradation kinetics and detoxification of an urban wastewater treatment plant effluent contaminated with pharmaceuticals, *Water Res.*, 43 (2009) 4070–4078.
- [12] L. Lloret, G. Eibes, T.A. Lu-Chau, M.T. Moreira, G. Feijoo, J.M. Lema, Laccase-catalyzed degradation of anti-inflammatories and estrogens, *Biochem. Eng. J.*, 51 (2010) 124–131.
- [13] S. Wu, L. Zhang, J. Chen, Paracetamol in the environment and its degradation by microorganism, *Appl. Microbiol. Biotechnol.*, 96 (2012) 875–884.
- [14] M. Isidori, M. Lavorgna, A. Nardelli, A. Parrella, L. Previtiera, M. Rubino, Ecotoxicity of naproxen and its phototransformation products, *Sci. Total Environ.*, 348 (2005) 93–101.
- [15] M. DellaGreca, M. Brigante, M. Isidori, A. Nardelli, L. Previtiera, M. Rubino, F. Temussi, Phototransformation and ecotoxicity of the drug Naproxen-Na, *Environ. Chem. Lett.*, 1 (2003) 237–241.
- [16] J.C. Morales-Mejía, R. Almanza, F. Gutiérrez, Solar photocatalytic oxidation of hydroxy phenols in a CPC reactor with thick TiO₂ films, *Energy Procedia*, 57 (2014) 597–606.
- [17] H.P. Baum, J.M. Gordon, Geometric characteristics of ideal non-imaging (CPC) solar collectors with cylindrical absorber, *Solar Energy*, 33 (1984) 455–458.
- [18] R. Winston, J.C. Miñano, P. Benitez, *Nonimaging Optics*, Elsevier, UK, 2005.
- [19] J.C. Morales-Mejía, R. Almanza, UVA Solar Irradiance on Inclined Surfaces 19.4° and Fixed in the South of Mexico City, XXXVIII National Solar Energy Week and XI Congress Iberoamerican, ANES, Congress Memories, Mexico, 2013.
- [20] W. Huang, M. Lei, H. Huang, J. Chen, H. Chen, Effect of polyethylene glycol on hydrophilic TiO₂ films: porosity-driven superhydrophilicity, *Surf. Coat. Technol.*, 204 (2010) 3954–3961.
- [21] J.C. Morales-Mejía, L. Angeles, R. Almanza, Synthesis and characterization of TiO₂ porous films for heterogeneous photocatalysis, *Comput. Water Energy Environ. Eng.*, 3 (2014) 36–40.
- [22] P. Novotna, J. Krysa, J. Maixner, P. Kluson, P. Novak, Photocatalytic activity of sol–gel TiO₂ thin films deposited on soda lime glass and soda lime glass precoated with a SiO₂ layer, *Surf. Coat. Technol.*, 204 (2010) 2570–2575.
- [23] B. Ohtani, O.O. Prieto-Mahaney, D. Li, R. Abe, What is Degussa (Evonik) P25? Crystalline composition analysis, reconstruction from isolated pure particles and photocatalytic activity test, *J. Photochem. Photobiol., A*, 216 (2010) 179–182.
- [24] J. Yu, H. Yu, B. Cheng, M. Zhou, X. Zhao, Enhanced photocatalytic activity of TiO₂ powder (P25) by hydrothermal treatment, *J. Mol. Catal. A*, 253 (2006) 112–118.
- [25] D.C. Hurum, A.G. Agrios, K.A. Gray, T. Rajh, M.C. Thurnauer, Explaining the enhanced photocatalytic activity of Degussa P25 mixed-phase TiO₂ using EPR, *J. Phys. Chem. B*, 107 (2003) 4545–4549.
- [26] APHA, AWWA, WEF, *Standard Methods for Examination of Water and Wastewater*, 22nd ed., APHA, USA, 2012.
- [27] R. Day, A. Underwood, *Quantitative Analysis*, 5th ed., Prentice-Hall Inc., USA, 2001.
- [28] L.J.D. Arsov, C. Kormann, W. Plieth, Electrochemical synthesis and in situ Raman spectroscopy of thin films of titanium dioxide, *J. Raman Spectrosc.*, 22 (1991) 573–575.
- [29] H.L. Ma, J.Y. Yang, Y. Dai, Y.B. Zhang, B. Lu, G.H. Ma, Raman study of phase transformation of TiO₂ rutile single crystal irradiated by infrared femtosecond laser, *Appl. Surf. Sci.*, 253 (2007) 7497–7500.
- [30] C.J. Howard, T.M. Sabine, F. Dickson, Structural and thermal parameters for rutile and anatase, *Acta Crystallogr., Sect. B*, 47 (1991) 462–468.
- [31] J.M. Herrmann, Photocatalysis fundamentals revisited to avoid several misconceptions, *Appl. Catal., B*, 99 (2010) 461–468.
- [32] E. Arany, R.K. Szabó, L. Apáti, T. Alapi, I. Iilsz, P. Mazellier, A. Dombi, K. Gajda-Schranz, Degradation of naproxen by UV, VUV photolysis and their combination, *J. Hazard. Mater.*, 262 (2013) 151–157.
- [33] R. Marotta, D. Spasiano, I. Di Somma, R. Andreozzi, Photodegradation of naproxen and its photoproducts in aqueous solution at 254 nm: a kinetic investigation, *Water Res.*, 47 (2013) 373–383.

- [34] K.A.K. Musa, L.A. Eriksson, Theoretical study of the phototoxicity of naproxen and the active form of nabumetone, *J. Phys. Chem. A*, 112 (2008) 10921–10930.
- [35] H. Zhang, P. Zhang, Y. Ji, J. Tian, Z. Du, Photocatalytic degradation of four non-steroidal anti-inflammatory drugs in water under visible light by P25-TiO₂/tetraethyl orthosilicate film and determination via ultra performance liquid chromatography electrospray tandem mass spectrometry, *Chem. Eng. J.*, 262 (2015) 1108–1115.
- [36] R.R. Giri, H. Ozaki, S. Ota, R. Takanami, S. Taniguchi, Degradation of common pharmaceuticals and personal care products in mixed solutions by advanced oxidation techniques, *Int. J. Environ. Sci. Technol.*, 7, (2010) 251–260.
- [37] A.Y.C. Tong, R. Braund, D.S. Warren, B.M. Peake, TiO₂-assisted photodegradation of pharmaceuticals – a review, *Cent. Eur. J. Chem.*, 10, (2012) 989–1027.
- [38] M.J. Benotti, B.D. Stanford, E.C. Wert, S.A. Snyder, Evaluation of a photocatalytic reactor membrane pilot system for the removal of pharmaceuticals and endocrine disrupting compounds from water, *Water Res.*, 43 (2009) 1513–1522.
- [39] N. Jallouli, K. Elghniji, O. Hentati, A.R. Ribeiro, A.M.T. Silva, M. Ksibi, UV and solar photo-degradation of naproxen: TiO₂ catalyst effect, reaction kinetics, products identification and toxicity assessment, *J. Hazard. Mater.*, 304 (2016) 329–336.
- [40] M. Isidori, M. Lavorgna, A. Nardelli, A. Parrella, L. Previtiera, M. Rubino, Ecotoxicity of naproxen and its phototransformation products, *Sci. Total Environ.*, 348 (2005) 93–101.